

Journal of Materials Chemistry A

Accepted Manuscript



This is an *Accepted Manuscript*, which has been through the Royal Society of Chemistry peer review process and has been accepted for publication.

Accepted Manuscripts are published online shortly after acceptance, before technical editing, formatting and proof reading. Using this free service, authors can make their results available to the community, in citable form, before we publish the edited article. We will replace this *Accepted Manuscript* with the edited and formatted *Advance Article* as soon as it is available.

You can find more information about *Accepted Manuscripts* in the [Information for Authors](#).

Please note that technical editing may introduce minor changes to the text and/or graphics, which may alter content. The journal's standard [Terms & Conditions](#) and the [Ethical guidelines](#) still apply. In no event shall the Royal Society of Chemistry be held responsible for any errors or omissions in this *Accepted Manuscript* or any consequences arising from the use of any information it contains.

Cite this: DOI: 10.1039/c0xx00000x

www.rsc.org/xxxxxx

ARTICLE TYPE

Three-dimensional hierarchical MoS₂ nanoflake arrays/carbon cloth as high-performance flexible lithium-ion battery anodes†

Hailong Yu,^{‡a} Chunling Zhu,^{‡b} Kai Zhang,^a Yujin Chen,^{*a} Chunyan Li,^a Peng Gao,^{*b} Piaoping Yang,^{*b} and Qiuyun Ouyang^a

Received (in XXX, XXX) Xth XXXXXXXXX 20XX, Accepted Xth XXXXXXXXX 20XX

DOI: 10.1039/b000000x

Flexible lithium-ion batteries are the key to powering a new generation of flexible electronics such as roll-up displays, smart electronics, and wearable devices. Here we report, for the first time, one-step hydrothermal synthesis of a three-dimensional (3D) hierarchical MoS₂ nanoflake arrays/carbon cloth which shows potential for improving the performance of flexible lithium-ion batteries. Structural characterizations show that the 3D hierarchical MoS₂ nanoflakes arrays/carbon cloth has a similar ordered woven structure to the bare carbon cloth. Each carbon microfiber is covered with many highly ordered MoS₂ nanoflake arrays, and the typical MoS₂ nanoflake, with expanded spacing of the (002) crystal plane, has a uniform width of about 400 nm and a thickness of less than 15 nm. The flexible 3D MoS₂ nanoflake arrays/carbon cloth as a flexible lithium-ion battery anode has a high reversible capacity of 3.0–3.5 mAh cm⁻² at a current density of 0.15 mA cm⁻² and outstanding rate discharging/charging stability. Moreover, the fabricated full battery, with commercial LiCoO₂ powder and the hierarchical architectures as electrodes, exhibits high flexibility and superior electrochemical performance, and can light a commercial red LED even after 50 cycles of bending the full battery.

1 Introduction

Recent advances in flexible and bendable electronics such as rollup displays, smart electronics, and wearable devices, promoted the development of flexible lithium-ion batteries (LIBs) due to their high power density.¹ Several kinds of flexible substrates used as electrodes have been developed. Electronically conducting polymers (ECPs), including polypyrrole, polyaniline, and polythiophene, are particularly interesting because these materials are inexpensive and bendable.^{2, 3} However, the main drawbacks with ECP-based batteries are, generally, their poor cycling stabilities, high self-discharge rates, and low capacities due to the insufficient doping levels and unstable doped states.^{2, 3} Recently, flexible electrodes based on inorganic materials, such as carbon nanotube (or graphene) paper, virus-templated Co₃O₄ nanowires, and TiO₂ cloths, have been developed, demonstrating their high capacity and good cycling stability.^{4–8} However, it is still a great challenge to fabricate highly flexible LIBs with both high mechanical strength and excellent electrochemical properties.

Carbon cloths, as a new kind of substrate, possess some advantageous properties over ECPs and other inorganic materials, including their high conductivity, high strength, and good corrosion resistance and, at the same time, are available commercially. Recently, some one-dimensional nanostructures grown on carbon cloths have been successfully achieved. Liu et al. fabricated hierarchical three-dimensional ZnCo₂O₄ nanowire

arrays/carbon cloth and used them to assemble a flexible LIB battery to power commercially available light-emitting diode (LED) and displays.⁹ Wang et al. grown TiO₂ nanorods on carbon cloths and obtained flexible TiO₂ cloths through a simple post-heating treatment process.¹⁰ The flexible TiO₂ cloths offers promising applications in many areas such as flexible electrodes of photoelectric devices, and recyclable photocatalysts.¹⁰ However, so far, only a few nanomaterials are able to grow successfully on carbon cloths, and then can be used as electrodes in flexible devices.

As a typical layered structure, MoS₂ has been extensively investigated as potential anodes in LIBs because of its spacing between neighboring layers (0.615 nm) and the weak van der Waals forces between the layers, allowing Li ions to readily diffuse without a significant increase in volume.^{11–15} Moreover, the rate capacity and long-term stability of MoS₂ could be significantly improved by several strategies including constructing MoS₂ based nanocomposites, growing MoS₂ nanostructures on conductive substrates, and expanding the spacing between neighboring layers.^{16–22} However, to the best of our knowledge, the exfoliated MoS₂ nanostructure-based flexible electrodes have not yet been reported.

We recently demonstrated the synthesis of three-dimensional (3D) hierarchical graphene/MoS₂ nanoflake arrays with large surface areas and porous structures.²² Due to the unique structures, the reversible discharging capacity is as high as 516 mAh g⁻¹ even at a high current density of 8 A g⁻¹. In the current work, we report the synthesis of 3D hierarchical MoS₂ nanoflake

arrays/carbon cloth through a one-step method without any surfactants. The 3D architecture as a LIBs anode exhibited ultrahigh capacity, excellent cycling performance, and good rate discharging/charging stability. Using the 3D MoS₂ nanoflake arrays/carbon cloth as a binder-free anode, flexible full LIBs were assembled, which showed excellent mechanical strength and electrochemical properties and could light a commercial LED even while the full LIB was repeatedly bended.

2 Experimental Section

2.1 Materials

Carbon cloth with hydrophilic surfaces was purchased from Tianjin Kermel Chemical Re-agent Co. Ltd. (Tianjin, China), and its through plate resistance was low than 5 mΩ cm⁻². The cathode (the LiCoO₂/Al foil) used as full battery was purchased from Shenyang Kejing Materials Technology Co., LTD, and loading amount of LiCoO₂ powder is about 150 g m⁻². All other reagents were analytically pure, and used without further purification.

2.2 Synthesis of MoS₂ nanoflake arrays/carbon cloth

The growth method of MoS₂ nanoflake arrays on carbon cloth is similar to the one reported by our previous literature.²² The sample CCMS-2 was fabricated as follows: carbon cloth (12 cm²) was dispersed into distilled water (15 mL) under ultrasonication for 30 min. Then, ethanol (25 mL), MoO₃ (60 mg), thiacetamide (70 mg), and urea (0.3 g) were added to the suspension under vigorous stirring. After stirring for 1 h, the mixture was then transferred into a Teflon-lined stainless steel autoclave with a capacity of 50 mL for hydrothermal treatment at 220 °C for 24 h. The autoclave was cooled to room temperature naturally, and then the carbon cloth coated with MoS₂ was washed with distilled water and absolute ethanol, and dried in a vacuum oven at 60 °C for 12 h. For comparison, CCMS-1 and CCMS-3 were prepared by changing the addition amount of MoO₃ precursor to 30 and 90 mg, respectively, under the same conditions described above.

2.3 Characterization

The morphology and size of the synthesized 3D hierarchical MoS₂ nanoflake arrays/carbon cloth were characterized by scanning electron microscope [HITACHI S-5200] and an FEI Tecnai-F20 transmission electron microscope equipped with a Gatan imaging filter (GIF). The crystal structure of the sample was determined by X-ray diffraction (XRD)[D/max 2550 V, Cu Kα radiation]. XPS measurements were carried out using a spectrometer with Mg Kα radiation (ESCALAB 250, Thermo Fisher Scientific Co.). The binding energy was calibrated with the C 1s position of contaminant carbon in the vacuum chamber of the XPS instrument (284.8 eV). Raman spectroscopy was performed on an inVia Renishaw Raman microscope (λ_e=488 nm). The mechanical strength of the 3D hierarchical MoS₂ nanoflake arrays/carbon cloth were measured by Zwick Materials Machine Z010 at room temperature and the carbon cloth composite was carefully cut into strips with a size of approximately 20 mm × 80 mm before the tensile test, and the initial tensile length of 30 mm and a drawing speed of 100 mm/min.

2.4 Electrode preparation and electrochemical measurements

The electrochemical performance of the as-synthesized MoS₂ nanoflake arrays/carbon cloth was investigated by using it as a binder-free anode in LIB in coin-type half-cells, which was laboratory-assembled by a CR2016 in an argon-filled glove box. A pure Li foil was used as the counter electrode. A piece of MoS₂ nanoflake arrays/carbon cloth was used as the working electrode without carbon black and any binder such as PVDF and PTFE. Celgard 2400 polymer separators were employed between the two electrodes. The electrolyte was made of LiPF₆ (1 M) in a mixture of ethylene carbonate (EC) and dimethyl carbonate (DMC) with the volume ratio 1:1. The cell was galvanostatically charged and discharged between 0.001 and 3.0 V versus Li⁺/Li at room temperature on a program-controlled test system.

2.5 Full battery assembly and electrochemical measurement

To make a full battery, the flexible MoS₂/carbon cloth and the LiCoO₂/Al foil are used as anode and cathode, respectively. Aluminum and copper foil as the current collectors were jointed to the side of cathode and anode electrodes, respectively. An aqueous solution of 1.0 mol L⁻¹ LiPF₆ in a mixture of ethylene carbonate (EC) and diethyl carbonate (DMC) (v/v = 1:1) served as the electrolyte and a Celgard 2400 membrane was used as the separator. Nickel foams were used as shims to help the current collectors contact with cathode and anode. The whole battery was packaged by Kapton boards with epoxy resin as adhesive in the glovebox with argon condition. The cells were galvanostatically charged and discharged between 1.0 and 4.1 V versus Li⁺/Li at room temperature on a program-controlled test system.

3 Results and discussion

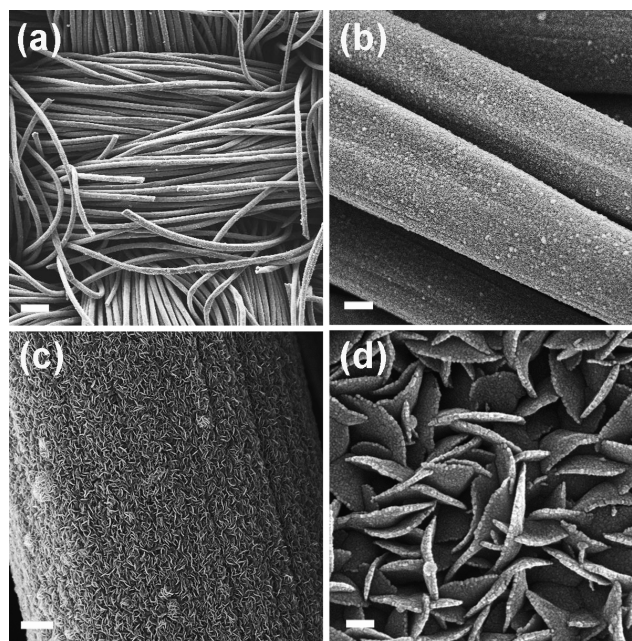


Figure 1. (a)-(d) Typical SEM images of 3D hierarchical MoS₂ nanoflake arrays/carbon cloth (CCMS-2) at different magnifications which is prepared by addition 60 mg MoO₃ precursor. Scale bars, a) 50 μm, b) 3 μm, c) 1 μm, d) 100 nm.

The obtained 3D hierarchical MoS₂ nanoflake arrays/carbon cloths with differing amount of MoO₃ precursor, 30 mg, 60 mg, and 90 mg, are denoted as CCMS-1, CCMS-2, and CCMS-3, respectively. The content of MoS₂ in these composites were determined by the method reported previously.⁹ Both the

Cite this: DOI: 10.1039/c0xx00000x

www.rsc.org/xxxxxx

ARTICLE TYPE

composites and bar carbon cloth were weighed in a high-precision analytical balance (Shimadzu, max weight 42 g, $d=0.01$ mg). The reading difference was the exact mass for the MoS₂ on carbon cloth. The loading densities of the MoS₂ active materials in CCMS-1, CCMS-2, and CCMS-3 are calculated as about 1.2, 1.6, 2.2 mg cm⁻², respectively.

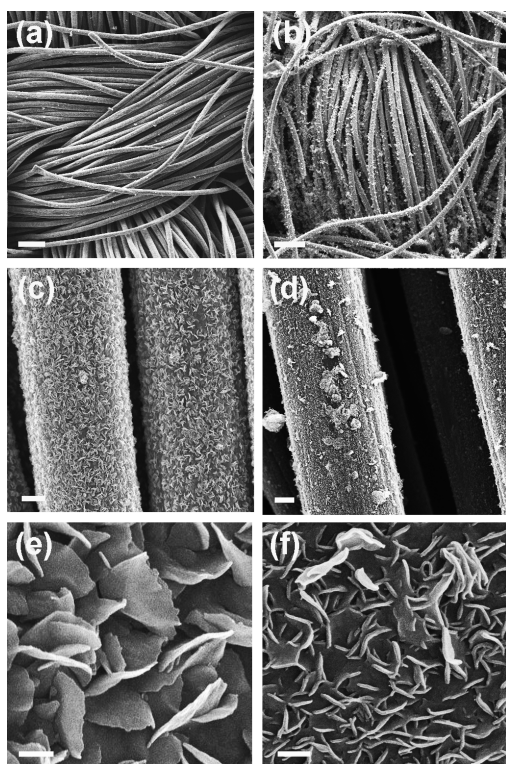


Figure 2. (a)-(f) Typical SEM images of 3D hierarchical MoS₂ nanoflake arrays/carbon cloth (CCMS-1 and CCMS-3) at different magnifications which is prepared by addition 30 mg (a, c, e) and 90 mg (b, d, f) of MoO₃ precursor. Scale bars, a) 50 μ m, b) 60 μ m, c) 2 μ m, d) 2 μ m, e) 200 nm f) 200 nm.

The morphology and the structure of the final product were investigated by scanning electron microscopy (SEM) and transmission electron microscopy (TEM) analyses. Figure 1(a) shows a low-magnification SEM image of CCMS-2. A similar ordered woven structure to the bare carbon cloth templates can be clearly seen. The 3D hierarchical MoS₂ nanoflakes arrays/carbon composite fibers have a uniform diameter of about 8.5 μ m, as shown in Figure 1(b). Figure 1(c) shows that each carbon microfiber is covered with numerous highly ordered 3D MoS₂ nanoflake arrays, and void space is presented among MoS₂ nanoflakes. Magnified MoS₂ nanoflakes have a uniform width of about 400 nm, as shown Figure 1(d).

Although the 3D hierarchical MoS₂ nanoflakes arrays/carbon was still obtained, we noted that the added amount of MoO₃ precursor had a very important effect on the density and size of the MoS₂ nanoflakes in the composite, as shown in Figure 2(a)

and (b). The density of MoS₂ nanoflakes grown on the carbon cloths increased with the increasing amount of the precursor, as shown in Figure 2(c) and (d). However, excessive addition of MoO₃ would lead to the deposition of large MoS₂ spheres on MoS₂ nanoflake arrays grown on the carbon fibers, as shown in Figure 2(d). The width of MoS₂ nanoflake is increased to 500–600 nm as 30 mg of MoO₃ precursor is added (Figure 2(e)), and is decreased to 200–400 nm if 90 mg of MoO₃ precursor is added (Figure 2(f)). Thus, the addition amount of MoO₃ precursor can be used to adjust the density and size of MoS₂ nanoflakes grown on the carbon fibers. Moreover, the 3D hierarchical MoS₂ nanoflake arrays/carbon demonstrates excellent flexibility and could be readily rolled up with an arbitrary angle (Figure S1, ESI). † The tensile strength of 3D MoS₂ nanoflake arrays/carbon cloth is evaluated to be 3.7 MPa, tested by Zwick Materials Machine Z010 at room temperature. This result reveals that the as-prepared 3D MoS₂ nanoflake arrays/carbon cloth is also of high strength. In addition, even after a long time of strong ultrasonication, MoS₂ nanoflakes are still strongly adhered to the surface of carbon cloth, indicating that there is strong interaction between carbon cloth and MoS₂ nanoflakes. Similar to the growth mechanism of MoS₂ nanosheets on graphene, ¹⁹ MoO₄²⁻ could tightly adsorb onto the carbon cloth due to the presence of functional groups such as hydroxyl groups on the surface of carbon cloth, and then reacts with thiocetamide to form MoS₂/carbon cloth composites.

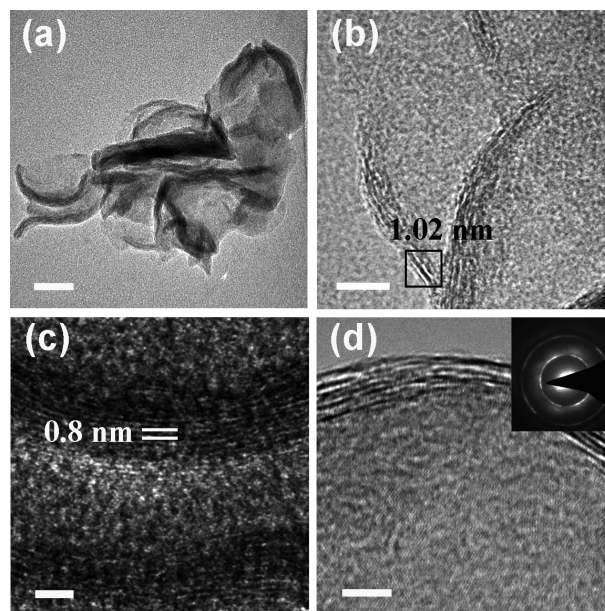


Figure 3. Structural characterization of MoS₂ nanoflakes. (a) Low-resolution TEM image, (b), (c) and (d) HRTEM images, the inset in (d) SAED pattern of MoS₂ nanoflakes. Scale bars, a) 50 nm, b) and c) 10 nm, and d) 5 nm.

Figure 3(a) shows a low-magnification TEM image of the MoS₂ nanoflakes with folded edges (sample CCMS-2). It can be seen that the rim of MoS₂ nanoflakes is thinner than the middle

parts. The high-resolution TEM (HRTEM) image demonstrates that the thickness of the MoS₂ nanoflakes is less than 15 nm, as shown in Figure 3(a)-(c). The small size will lead to more edges exposed to environments with higher chemical activity.²³⁻²⁴ Furthermore, the interlayer distance of (002) crystal plane of MoS₂ nanoflakes at most of the rim regions (marked by a black frame) measured from HRTEM image is about 1.02 nm (Figure 3(b)), and, at the middle regions, the value is about 0.8 nm (Figure 3(c)). The interlayer distance of the (002) plane of the MoS₂ nanoflakes varies from 0.8 nm at middle regions to 1.02 nm at rim regions. In contrast, the bulk MoS₂ materials have an interlayer distance of the (002) plane of 0.616 nm. The results reveal that the spacing of the (002) crystal plane of MoS₂ nanoflakes on the carbon fibers is significantly expanded. Top view of the (002) crystal plane of MoS₂ from HRTEM images (Figure 3(d)) and the selected-area electron diffraction pattern (the inset in Figure 3(d)) show the polycrystalline structure of the MoS₂ nanoflakes.²²

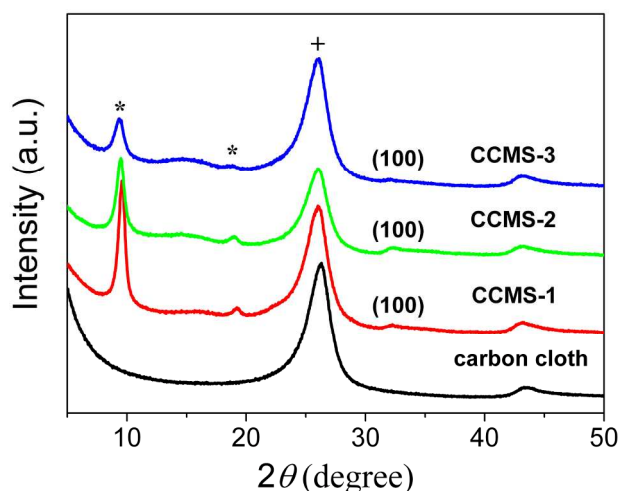


Figure 4. XRD patterns of carbon cloth, CCMS-1, CCMS-2 and CCMS-3

The exfoliated MoS₂ is further confirmed by X-ray diffraction (XRD) measurements. Figure 4 shows XRD patterns of CCMS-1, CCMS-2, CCMS-3, and carbon cloth. In the patterns of CCMS-1, CCMS-2, and CCMS-3, the diffraction peaks at $2\theta = 26.2$ and 43.4° come from carbon cloth, whereas the one at $2\theta = 32.6^\circ$ corresponds to the (100) crystal plane of MoS₂ (JPCDS No. 37-1492). It should be noted that the peak at $2\theta = 14.4^\circ$ corresponding to the (002) plane of the bulk MoS₂ could not be found. However, two new diffraction peaks centered at $2\theta = 9.4$ and 19.0° are observed, and their lattice spacings are calculated to be 0.94 and 0.47 nm, respectively, using the Bragg equation. The 2θ of the (002) diffraction peak is shifted to a low-angle of 9.4° , revealing an expanded interlayer distance of the (002) plane of 0.94 nm, which coincides with the HRTEM measured result (0.8–1.02 nm).^{23, 24, 25, 26} The diffraction peaks at $2\theta = 9.4$ and 19.0° are not presented in the XRD pattern of carbon cloth that was hydrothermally treated under the same conditions as CCMS-2 without Mo source (Figure S2). This reveals that expanded interlayer distance of the (002) plane of MoS₂ nanoflakes do not arise from the alkaline solvent in the reaction system. The expanded interlayer distance, smaller size, and more exposed

edges of the MoS₂ nanoflakes are beneficial to the enhanced electrochemical performance of the 3D hierarchical MoS₂ nanoflake arrays/carbon cloth.²¹

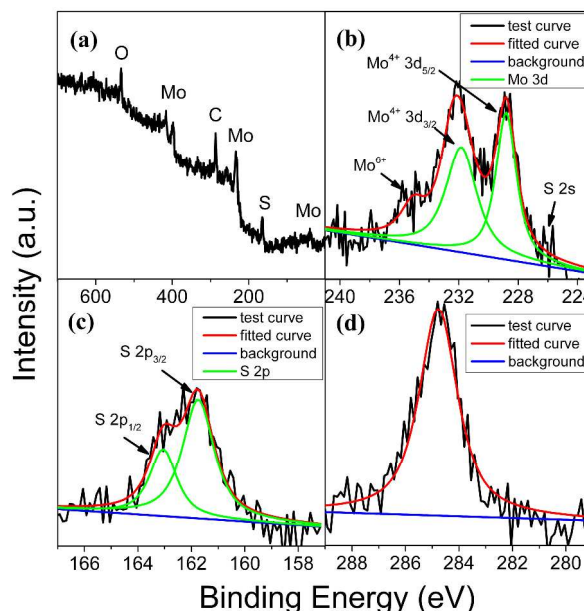


Figure 5. The XPS spectra of the 3D hierarchical MoS₂ nanoflake arrays/carbon cloth. (a) The survey XPS spectrum, (b) the Mo 3d XPS spectrum, (c) S 2p XPS spectrum, and (d) C 1s XPS spectrum.

The surface electronic state and composition of CCMS-2 were investigated by X-ray photoelectron spectroscopy (XPS) analysis. The survey XPS spectrum indicates that the 3D architectures contain element C, Mo, S, and O, as shown in Figure 5(a). Figure 5(b) shows a high-resolution spectrum in the binding energy range of 223–241 eV. The peaks at 228.8 eV and 231.9 eV correspond to the Mo⁴⁺ 3d_{5/2} and Mo⁴⁺ 3d_{3/2} components of MoS₂, respectively. The 3d_{5/2} and 3d_{3/2} peaks have separation energies close to 3.1 eV, characteristic of Mo species.²⁷⁻³⁵ The presence of a weak peak at around 235.8 eV, assigned to Mo⁶⁺ 3d_{5/2}, suggests that the oxidation of Mo is minimal.²⁷ The peak at around 226 eV corresponds to the S 2s component of MoS₂.^{34, 35} In the high-resolution S 2p spectra shown in Figure 5(c), the peaks at 161.7 eV and 163.0 eV are observed, corresponding to S²⁻ 2p_{3/2} and S²⁻ 2p_{1/2}, respectively. The intensity ratio of the characteristic peaks is about 2:1, and their separation energies is about 1.2 eV, which are typical characteristics of S²⁻ species. Furthermore, compared with the 2p_{3/2} (164.1 eV) and 2p_{1/2} (165.2 eV) peaks of elemental S, the peaks have negative binding energy shifts of about 2.3 eV, which is the typical 2p shift for S in MoS₂.²⁹⁻³⁷ Figure 5(d) shows the standard carbon peak at 284.8 eV.

The presence of MoS₂ in the final product is further confirmed by Raman measurement (Figure S3).[†] The peaks at 379 cm⁻¹ and 407 cm⁻¹, ascribed to E_g¹ and A_g¹ respectively, are typically characteristic peaks of hexagonal MoS₂.^{32, 33} An energy-dispersive X-ray (EDX) pattern (Figure S4) demonstrates that the final product contains a small quantity of O besides C, Mo, and S.[†] The calculated atomic ratio of S to Mo element is about 1.95, very close to the stoichiometric MoS₂. The C element comes from the carbon cloths and the Cu from the copper grid used to support the sample. The XPS, EDX and Raman measurements

Cite this: DOI: 10.1039/c0xx00000x

www.rsc.org/xxxxxx

ARTICLE TYPE

clearly show that the Mo element mainly exist in the form of MoS_2 in the final composite.

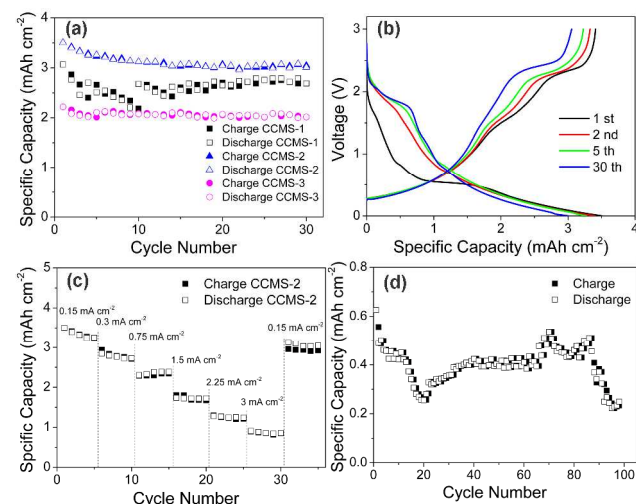


Figure 6. Electrochemical performance of 3D MoS_2 nanoflake arrays/carbon cloth. (a) Cycling performance of CCMS-1, CCMS-2, and CCMS-3, showing the reversible capacity value of 3.00 mAh cm^{-2} after 30 cycles with a coulombic efficiency of 97.6%. (b) typical voltage versus specific capacity profiles for the first first, second, fifth and 15th discharge/charge-cycle, (c) rate performance of CCMS-2, and (d) the capacity of carbon cloth as electrode at 0.15 mA cm^{-2} .

The interesting 3D hierarchical architectures, composed of carbon cloth with high conductivity and MoS_2 nanoflake arrays with void spaces, and the expanded (002) crystal plane, are promising for high-performance LIB anodes.^{20-23, 27} We first assembled half-cells using the 3D hierarchical architectures and pure Li foil as electrodes. Figure 6(a) shows the discharge/charge capacities and cyclic stability of CCMS-1, CCMS-2, and CCMS-3 at a low current density of 0.15 mA cm^{-2} . CCMS-1, CCMS-2, and CCMS-3 have nearly ideal coulombic efficiencies of 93.5%, 97.6%, and 97.3%, respectively, substantially higher than any other anode.^{30, 38, 39, 40, 41} Their first discharge capacities are 3.1, 3.5, and 2.2 mAh cm^{-2} , respectively. After 30 cycles, the capacities become 2.7, 3.0, and 2.0 mAh cm^{-2} , respectively, suggesting that the 3D hierarchical MoS_2 nanoflake arrays/carbon cloth has good cycling stability at a low current density. Among the composites, CCMS-3 exhibits relatively low capacities, which may be ascribed to the presence of relatively large MoS_2 spheres in the sample.

Figure 6(b) shows voltage-capacity curves of the CCMS-2 at a low current density of 0.15 mA cm^{-2} for the first, second, 15th, and 30th charge/discharge cycles, respectively. In the initial discharge process, two clear voltage plateaus, at about 0.8 and 0.5 V, are observed. For the bulk MoS_2 , the plateau at 1.1 V is usually present in the initial lithiation process, resulting from the insertion of Li ions into the layer-to-layer of MoS_2 .¹¹ However, for the MoS_2 nanoflakes obtained in this work, the

potential plateau shifts to 0.8 V. This is attributed to the presence of the defective sites in nanostructured MoS_2 induced by the small size effect.³⁸⁻⁴⁰ These defective sites allow additional Li ions to travel through the expanded MoS_2 nanoflakes and leads to the formation of Li_xMoS_2 .³⁸⁻⁴⁰ The plateau at 0.5 V can be attributed to a conversion reaction process, which first entails the in situ decomposition of MoS_2 into Mo particles embedded into a Li_2S matrix and then the formation of a gel-like polymeric layer resulting from electrochemically driven electrolyte degradation. This process makes the charging capacity decrease during the following cycle.⁴¹⁻⁴⁵ In the following discharge processes, two potential plateaus of reduction peaks at 2.2 and 0.9 V are observed, and the plateau at 0.5 V disappears, which agrees well with the reported lithiation profiles of MoS_2 .^{33, 44} In addition, an oxidation peak located at about 2.3 V is also observed during the charge processes, which is attributed to oxidation of Li_2S .

Due to their unique architectures, the 3D hierarchical MoS_2 nanoflake arrays/carbon cloth anode exhibits very good rate performances, as shown in Figure 6(c). The discharge capacities are 3.26, 2.73, 2.39, 1.72, 1.24, and 0.85 mAh cm^{-2} at the current densities of 0.15, 0.3, 0.75, 1.5, 2.25, and 3.0 mA cm^{-2} , respectively. It is worth noting that even at the current density rate of 3.0 mA cm^{-2} , the reversible capacity is still retained at 0.85 mAh cm^{-2} after 5 cycles. Moreover, the capacity is still reversible back to 3.05 mAh cm^{-2} once the charging/discharging current density is set back to 0.15 mA cm^{-2} after the charge/discharge processes. As a result, the 3D hierarchical MoS_2 nanoflake arrays/carbon cloth exhibits high specific capacity, high coulombic efficiency, good cycling stability, and outstanding rate performance, offering a very promising potential for application in the flexible battery.

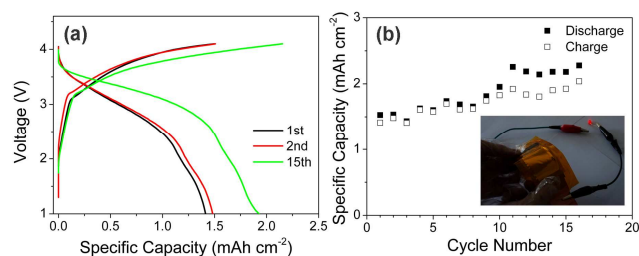


Figure 7. Electrochemical performance of flexible full battery. (a) The voltage versus specific capacity profiles of full flexible battery for the first, second, and 15th discharge/charge cycles, (b) the cycling performance of full battery, and inset: The flexible full battery can lighten a red LED even after 50 cycles of bending the full battery.

It should be noted that the carbon cloth exhibits a negligible contribution to the total capacity of the 3D MoS_2 nanoflake arrays/carbon anode. As shown in Figure 6(d), the specific capacity is about 0.4 mAh cm^{-2} at the current density of 0.15 mA cm^{-2} , which is much less than that of the 3D MoS_2 nanoflake arrays/carbon cloth. The size of the carbon cloth fibers is relatively large and the carbon fibers have no pores on the surfaces, leading to the insertion and deintercalation of Li on the

surface of the carbon fibers. The MoS₂ nanoflakes, grown on the surfaces of the carbon fibers, will act as the Li insertion and deintercalation reaction sites, enhancing overall capacity as a consequence. Therefore, the contribution of carbon cloth to the total capacity of the 3D hierarchical nanostructures is negligible, but its high conductivity plays an important role in the good stability of the anodes. In addition, MoS₂ flowers with a diameter of about 1 μm were prepared without substrates such as carbon cloth in the reaction system, described in our previous work.²² The capacity of the MoS₂ flowers is about 0.357 mAh cm⁻² at 0.15 mA cm⁻², lower than that of 3D hierarchical MoS₂ nanoflake arrays/carbon cloth.²²

As described above, the flexible 3D hierarchical MoS₂ nanoflake arrays/carbon cloth demonstrates excellent electrochemical performance. The excellence could be attributed to (1) the expanded (002) crystal plane of the MoS₂ nanoflakes, which provides sufficient space for a high rate of lithium intercalation; (2) the presence of highly conductive carbon cloth, which greatly improves the conductivity of the 3D architectures and facilitates rapid electron transport during the Li insertion/extraction reaction; (3) the thinness of the MoS₂ nanoflakes (less than 15 nm), which provides a shorter pathway for Li-ion diffusion and requires a lower activation energy for the Li-ion intercalation reaction,^{9, 17, 21, 22} (4) the unique structure of the 3D MoS₂ nanoflake arrays/carbon cloth, which affords a higher rate of performance. The woven carbon cloth is favorable for the formation of loose textures in the MoS₂ nanoflake arrays/carbon cloth anode, which buffers the mechanical stress and volume variation accompanying the lithium charging/discharging process,^{9, 19, 21, 22} (5) the void spaces between the neighboring MoS₂ nanoflake arrays, which makes the electrolyte contact efficiently with the 3D architectures and provides more reactive sites for Li-ion intercalation, and, thus, enhances the reversibility of the anode significantly.^{22, 46, 47}

The excellent electrochemical performance of the 3D MoS₂ nanoflake arrays/carbon cloth combined with high flexible mechanical characteristics make it an ideal candidate as an anode of a flexible Lithium ion full battery. The structure of the fabricated flexible full battery is shown in Figure S5 †. It consists of the flexible 3D MoS₂ nanoflake arrays/carbon cloth as the anode, a flexible separator, a commercial LiCoO₂/Al foil as the cathode, LiPF₆-based electrolyte, nickel foam as shims, and a flexible Kapton board shell. Figure 7(a) presents the voltage-capacity profiles of the as-prepared flexible full battery device for the first, second, and 15th charge/discharge cycles at a current rate of 0.15 mA cm⁻² in the voltage window of 1.0–4.1 V. It can be observed that the potential plateau is between the range of 2.3 and 3.7 V in the initial discharge progress, and slightly increased after the second cycle.⁴¹ The specific capacity is much lower than that of the half cell. This is the result of the lower capacity of the LiCoO₂ cathode, which does not fit well with the anode capacity. The initial discharge capacity of the full cell is about 1.41 mAh cm⁻² (Figure 7(a)), and the reversible discharge capacity is increased, gradually, after the second cycle (Figure 7(b)). This may be attributed to the fact that the electrodes are infiltrated completely after the second cycle. Furthermore, the full cell has little change in the capacities under bending angle of 45 and 60 degree. To demonstrate its practical applications and its durability

to sustain mechanical stress, we used the as-assembled full battery to power a commercial red LED light. As shown in the inset of Figure 7(b), the red LED can be lit even after 50 cycles of bending the full battery.

4 Conclusions

A process was developed to synthesize 3D hierarchical MoS₂ nanoflake arrays/carbon cloth, in which the spacing of the (002) crystal plane was significantly expanded. The 3D hierarchical MoS₂ nanoflake arrays/carbon cloth as a lithium ion battery anode exhibited high specific capacity, high coulombic efficiency, good cycling stability, and outstanding rate performance. We fabricated a flexible full battery with the flexible 3D hierarchical MoS₂ nanoflake arrays/carbon cloth-anode and LiCoO₂-cathode, demonstrating excellent electrochemical performance and mechanical stability against external bending stress. Even after 50 cycles of continuous bending, the full battery can still be used to power a commercial red LED light. The bendable battery, with excellent electrochemical performances, could be used in the next generation of electronic devices such as rollup displays, smart electronics, and wearable devices.

Acknowledgments

We thank the National Natural Science Foundation of China (Grant Nos. 51272050, 61205113, 21171045 and 21001035), Program for New Century Excellent Talents in University (NECT-10-0049) for the financial support of this research, and also the 111 project (B13015) of Ministry Education of China to the Harbin Engineering University.

Notes and references

^a Key Laboratory of In-Fiber Integrated Optics, Ministry of Education, and College of Science, Harbin Engineering University, Harbin 150001, Heilongjiang, China. Fax: 86-451-82519754; Tel: 86-451-82519754; E-mail: chen yujin@hrbeu.edu.cn

^b College of Materials Science and Chemical Engineering, Harbin Engineering University, Harbin, Heilongjiang, 150001, China. E-mail: gaopeng@hrbeu.edu.cn, and yangpiaoping@hrbeu.edu.cn

† Electronic Supplementary Information (ESI) available: [Photographic image of the 3D hierarchical MoS₂ nanoflake arrays/carbon cloth, XRD pattern of carbon cloth that was hydrothermally treated under the same conditions as CCMS-2 without Mo source, Raman spectra and EDS pattern of the 3D hierarchical MoS₂ nanoflake arrays/carbon cloth and carbon cloth, and photograph of a flexible full battery based on MoS₂ nanoflake arrays/carbon cloth-liquid electrolyte-LiCoO₂ full battery]. See DOI: 10.1039/b000000x/

‡ These authors contributed equally to this work.

- J. A. Rogers, T. Someya and Y. G. Huang, *Science*, 2010, **327**, 1603.
- H. Nishide and K. Oyaizu, *Science*, 2008, **319**, 737.
- L. Nyholm, G. Nyström, A. Mihranyan and M. Strømme, *Adv. Mater.*, 2011, **23**, 3751.
- R. Elazari, G. Salitra, A. Garsuch, A. Panchenko and D. Aurbach, *Adv. Mater.*, 2011, **23**, 5641.
- X. L. Jia, C. Z. Yan, Z. Chen, R. R. Wang, Q. Z. Zhang, L. G. Guo, F. Wei and Y. F. Lu, *Chem. Commun.*, 2011, **47**, 9669.
- L. Jabbour, C. Gerbaldi, D. Chaussy, E. Zeno, S. Bodoardo and D. Beneventi, *J. Mater. Chem.*, 2010, **20**, 7344.
- H. Gwon, H. S. Kim, K. U. Lee, D. H. Seo, Y. C. Park, Y. S. Lee, B. T. Ahn and K. Kang, *Energy Environ. Sci.*, 2011, **4**, 1277.

Cite this: DOI: 10.1039/c0xx00000x

www.rsc.org/xxxxxx

ARTICLE TYPE

- 8 K. T. Nam, D. W. Kim, P. J. Yoo, C. Y. Chiang, N. Meethong, P. T. Hammond, Y. M. Chiang and A. M. Belcher, *Science*, 2006, **312**, 885.
- 9 B. Liu, J. Zhang, X. F. Wang, G. Chen, D. Chen, C. W. Zhou and G. Z. Shen, *Nano Lett.*, 2012, **12**, 3005.
- 5 10 Z. R. Wang, H. Wang, B. Liu, W. Z. Qiu, J. Zhang, S. H. Ran, H. T. Huang, J. Xu, H. W. Han, D. Chen and G. Z. Shen, *ACS Nano*, 2011, **5**, 8412.
- 11 R. Shidpoura and M. Manteghian, *Nanoscale*, 2010, **2**, 1429.
- 12 C. Q. Feng, J. Ma, H. Li, R. Zeng, Z. P. Guo and H. K. Liu, *Mater. Res. Bull.*, 2009, **44**, 1811.
- 10 13 H. Hwang, H. Kim and J. Cho, *Nano Lett.*, 2011, **11**, 4826.
- 14 S. J. Ding, D. Y. Zhang, J. S. Chen and X. W. Lou, *Nanoscale*, 2012, **4**, 95.
- 15 G. D. Du, Z. P. Guo, S. Q. Wang, R. Zeng, Z. X. Chen and H. K. Liu, *Chem. Commun.*, 2010, **46**, 1106.
- 15 16 K. Chang, W. X. Chen, L. Ma, H. Li, H. Li, F. H. Huang, Z. D. Xu and Q. B. Zhang, *J. Mater. Chem.*, 2011, **21**, 17175.
- 17 K. Chang and W. X. Chen, *ACS Nano*, 2011, **5**, 4720.
- 18 K. Chang, W. X. Chen, L. Ma, H. Li, H. Li, F. H. Huang, Z. D. Xu, Q. B. Zhang and J. Y. Lee, *J. Mater. Chem.*, 2011, **21**, 6251.
- 20 19 K. Chang and W. X. Chen, *Chem. Commun.*, 2011, **47**, 4252.
- 20 J. Xiao, D. Choi, L. Cosimbescu, P. Koech, J. Liu and J. P. Lemmon, *Chem. Mater.*, 2010, **22**, 4522.
- 21 H. Liu, D. W. Su, R. F. Zhou, C. X. Wang and S. Z. Qiao, *Adv. Energy Mater.*, 2012, **2**, 970.
- 25 22 H. L. Yu, C. Ma, B. H. Ge, Y. J. Chen, Z. Xu, C. L. Zhu, C. Y. Li, Q. Y. Ouyang, P. Gao, J. Q. Li, C. W. Sun, L. H. Qi, Y. M. Wang and F. H. Li, *Chem. Eur. J.*, 2013, **19**, 5818.
- 23 H. S. S. Ramakrishna Matte, A. Gomathi, A. K. Manna, D. J. Late, R. Datta, S. K. Pati and C. N. R. Rao, *Angew. Chem. Int. Ed.*, 2010, **49**, 4059.
- 30 24 L. Ye, C. Z. Wu, W. Guo and Y. Xie, *Chem. Commun.*, 2006, **45**, 4738.
- 25 M. R. Gao, W. T. Yao, H. B. Yao and S. H. Yu, *J. Am. Chem. Soc.*, 2009, **131**, 7486.
- 35 26 K. Chang, W. Chen, L. Ma, H. Li, F. Huang, Z. Xu, Q. Zhang and J. Y. Lee, *J. Mater. Chem.*, 2011, **21**, 6251.
- 27 J. Kibsgaard, Z. B. Chen, B. N. Reinecke and T. F. Jaramillo, *Nat. Mater.*, 2012, **11**, 963.
- 40 28 Y. G. Li, H. L. Wang, L. M. Xie, Y. G. Liang, G. Hong and H. J. Dai, *J. Am. Chem. Soc.*, 2009, **131**, 15939.
- 29 J. S. Zabinski, M. S. Donley, S. D. Walck, T. R. Schneider and N. T. McDevitt, *Tribol. Trans.*, 1995, **38**, 894.
- 30 J. R. Lince, *J. Mater. Res.*, 1990, **5**, 895.
- 45 31 H. W. Wang, P. Skeldon and G. E. Thompson, *Surf. Coat. Technol.*, 1997, **91**, 200.
- 32 J. Xiao, X. J. Wang, X. Q. Yang, S. D. Xun, G. Liu, P. K. Koech, J. Liu and J. P. Lemmon, *Adv. Funct. Mater.*, 2011, **21**, 2840.
- 33 T. A. Patterson, J. C. Carver, D. E. Leyden and D. M. Hercules, *J. Phys. Chem.*, 1976, **80**, 1700.
- 50 34 V. O. Koroteev, L. G. Bulusheva, I. P. Asanov, E. V. Shlyakhova, D. V. Vyalikh and A. V. Okotrub, *J. Phys. Chem. C*, 2011, **115**, 21199.
- 35 G. Eda, H. Yamaguchi, D. Voiry, T. Fujita, M. W. Chen and M. Chhowalla, *Nano Lett.*, 2011, **11**, 5111.
- 55 36 T. J. Wieting and J. L. Verble, *Phys. Rev. B*, 1971, **3**, 4286.
- 37 G. L. Frey and R. Tenne, *Phys. Rev. B*, 1999, **60**, 2883.
- 38 R. Dominko, D. Arcon, A. Mrzel, A. Zorko, P. Cevc, P. Venturini, M. Gaberscek, M. Remskar and D. Mihailovic, *Adv. Mater.*, 2002, **14**, 1531.
- 60 39 G. X. Wang, S. Bewlay, J. Yao, H. K. Liu and S. K. Dou, *Electrochem. Solid-State Lett.*, 2004, **7**, A321.
- 40 R. Shidpour and M. Manteghian, *Nanoscale*, 2010, **2**, 1429.
- 41 Y. MiKi, D. Nakazato, H. Ikuta, T. Uchida and M. Wakihara, *J. Power Sources*, 1995, **54**, 508.
- 65 42 S. E. Cheon, K. S. Ko, J. H. Cho, S. W. Kim, E. Y. Chin and H. T. Kim, *J. Electrochem. Soc.*, 2003, **150**, A800.
- 43 J. Wang, J. Yang, C. Wan, K. Du, J. Xie and N. Xu, *Adv. Funct. Mater.*, 2003, **13**, 487.
- 44 J. Xiao, D. W. Choi, L. Cosimbescu, P. Koech, J. Liu and J. P. Lemmon, *Chem. Mater.*, 2010, **22**, 4522.
- 70 45 J. B. Goodenough, *J. Solid State Electrochem.*, 2012, **16**, 2019.
- 46 L. F. Hu, Z. L. Tang and Z. T. Zhang, *J. Power Sources*, 2007, **166**, 226.
- 47 L. F. Hu, R. Z. Ma, T. C. Ozawa and T. Sasak, *Inorg. Chem.*, 2010, **49**, 2960.
- 75